

## Even-in-magnetic-field part of transverse resistivity as a probe of magnetic order

Antonin Badura, Dominik Kriegner, Eva Schmoranzerová, Karel Výborný, Miina Leiviskä, Rafael Lopes Seeger, Vincent Baltz, Daniel Scheffler, Sebastian Beckert, Ismaila Kounta, et al.

#### ▶ To cite this version:

Antonin Badura, Dominik Kriegner, Eva Schmoranzerová, Karel Výborný, Miina Leiviskä, et al.. Even-in-magnetic-field part of transverse resistivity as a probe of magnetic order. 2024. hal-04376122

HAL Id: hal-04376122 https://hal.science/hal-04376122

Preprint submitted on 6 Jan 2024

**HAL** is a multi-disciplinary open access archive for the deposit and dissemination of scientific research documents, whether they are published or not. The documents may come from teaching and research institutions in France or abroad, or from public or private research centers.

L'archive ouverte pluridisciplinaire **HAL**, est destinée au dépôt et à la diffusion de documents scientifiques de niveau recherche, publiés ou non, émanant des établissements d'enseignement et de recherche français ou étrangers, des laboratoires publics ou privés.

# Even-in-magnetic-field part of transverse resistivity as a probe of magnetic order

Antonin Badura,<sup>1,2</sup> Dominik Kriegner,<sup>2,3</sup> Eva Schmoranzerová,<sup>1</sup> Karel Výborný,<sup>2</sup> Miina Leiviskä,<sup>4</sup> Rafael Lopes Seeger,<sup>4</sup> Vincent Baltz,<sup>4</sup> Daniel Scheffler,<sup>3</sup> Sebastian Beckert,<sup>3</sup> Ismaila Kounta,<sup>5</sup> Lisa Michez,<sup>5</sup> Libor Šmejkal,<sup>6,2</sup> Jairo Sinova,<sup>6,2</sup> Sebastian T. B. Goennenwein,<sup>7</sup> Jakub Železný,<sup>2</sup> and Helena Reichlová<sup>2,3</sup>

<sup>1</sup>Department of Chemical Physics and Optics,
Faculty of Mathematics and Physics, Charles University,
Ke Karlovu 5, 121 16 Prague 2, Czech Republic

<sup>2</sup>Institute of Physics, Czech Academy of Sciences,
Cukrovarnická 10, 162 53, Praha 6, Czech Republic

<sup>3</sup>Institut für Festkörper- und Materialphysik,
Technische Universität Dresden, 01062 Dresden, Germany

<sup>4</sup>Univ. Grenoble Alpes, CNRS, CEA,
Grenoble INP, Spintec, F-38000 Grenoble, France

<sup>5</sup>Aix-Marseille University, CNRS, CINaM, Marseille, France

<sup>5</sup>Aix-Marseille University, CNRS, CINaM, Marseille, France <sup>6</sup>Institut für Physik, Johannes Gutenberg Universität Mainz, 55128 Mainz, Germany <sup>7</sup>Universität Konstanz, Fachbereich Physik, 78457 Konstanz, Germany

#### Abstract

The detection of a voltage transverse to both an applied current and a magnetic field is one of the most common characterization techniques in solid-state physics. The corresponding component of the resistivity tensor  $\rho_{ij}$  can be separated into odd and even parts with respect to the applied magnetic field. The former contains information, for example, about the ordinary or anomalous Hall effect. The latter is typically ascribed to experimental artefacts and ignored. We here show that upon suppressing these artefacts in carefully controlled experiments, useful information remains. We first investigate the well-explored ferromagnet CoFeB, where the even part of  $\rho_{yx}$  contains a contribution from the anisotropic magnetoresistance, which we confirm by Stoner-Wohlfarth modelling. We then apply our approach to magnetotransport measurements in Mn<sub>5</sub>Si<sub>3</sub> thin films with a complex compensated magnetic order. In this material, the even part of the transverse signal is sizable only in the low-spin-symmetry phase below  $\approx 80$  K and thus offers a simple and readily available probe of the magnetic order.

#### I. INTRODUCTION

The electrical resistivity tensor  $\bar{\rho}$  is defined as  $\mathbf{E} = \bar{\rho}\mathbf{j}$ , where  $\mathbf{j}$  and  $\mathbf{E}$  are the current density and electric field vectors. The measurement of  $\bar{\rho}$  as a function of the applied external magnetic field is a fundamental characterization tool in solid-state physics. When performed on lithographically defined thin-film microstructures, it allows disentangling the different components of the resistivity tensor and relating them to particular physical phenomena, such as magnetoresistance and the different Hall effects [1, 2].

Components of the resistivity tensor  $\bar{\rho}$  are usually classified based on how they transform when the magnetic field  $\boldsymbol{H}$  or magnetic moments are reversed [3, 4]. The so-called Onsager relations state that  $\rho_{ij}(\boldsymbol{H},\boldsymbol{M})=\rho_{ji}(-\boldsymbol{H},-\boldsymbol{M})$ . Here for simplicity,  $\boldsymbol{M}$  denotes the generalized magnetic order vector of the system (such as magnetization or the Néel vector). The reversal of both the external magnetic field and all magnetic moments corresponds to the time-reversal symmetry (TRS). From the Onsager relations, it follows that the symmetric components of the resistivity tensor  $(\rho_{ij}^S = \rho_{ji}^S)$  are even under time-reversal, whereas the antisymmetric components  $(\rho_{ij}^A = -\rho_{ji}^A)$  are odd. The antisymmetric components can thus occur only when the time-reversal symmetry is broken. When TRS is broken by an external magnetic field, it results in the ordinary Hall effect, which is commonly used to determine the carrier type and density [5]. In a material with spontaneously broken TRS, the antisymmetric terms can be non-zero also in zero magnetic field. This leads to a variety of anomalous Hall effects [1, 6–8] in magnetically ordered materials, or topological Hall effects [9, 10] arising from a non-zero spin chirality.

In contrast, the symmetric components of the resistivity tensor can exist in all materials. In both magnetic and non-magnetic materials, the symmetric components typically depend directly on the external magnetic field, which we will refer to as ordinary magnetoresistance (OMR) [11]. In magnetic materials with finite spin-orbit coupling, the symmetric components will also depend on the orientation of the magnetic order, which is known as anisotropic magnetoresistance (AMR) [2]. Unlike the anomalous Hall effect, AMR is allowed by symmetry in all magnetic materials [12].

The various contributions to resistivity can thus be, in principle, distinguished by their relation to the symmetric or antisymmetric components of the resistivity tensor. Unfortunately, doing this experimentally is not straightforward. Instead, different contributions are

separated based on their odd/even symmetry with respect to the external magnetic field. Although the anomalous Hall effect or the AMR do not directly depend on the applied magnetic field, their experimental detection does, since the external magnetic field controls the magnetic order. However, this makes the interpretation of the results complicated since the effects that depend on the magnetic field directly (such as the OMR) can mix with the effects that depend on it indirectly. Furthermore, effects that rely directly on both the magnetic order and the magnetic field can also exist [13].

Experimentally, the different elements of the resistivity tensor are usually calculated from the voltage measured along and perpendicular to the current direction. For example, if a current applied along the x-axis induces finite voltage along the y-axis, then  $\rho_{yx}$  is non-zero. Hereafter, we shall use the terms longitudinal and transverse resistivity to refer to the signal measured in the respective orientation to the current flow. Note that these do not necessarily correspond to the diagonal and off-diagonal components of the resistivity tensor expressed in crystallographic axes since the current may flow in a general direction.

In the following, we summarize the effects which can result in a finite contribution to transverse resistivity and discuss their symmetry with respect to the applied magnetic field. The AHE contribution is an odd function of the applied magnetic field when the material is magnetically saturated. Similarly, in saturation, AMR has an even dependence on the magnetic field. However, when the magnetic saturation is not reached, there might be odd contributions arising from AMR and, vice versa, even contributions due to the AHE. That is because the reversal of the magnetic field does not result in the reversal of the magnetic order [14] while the Onsager relations only constrain the diagonal components of  $\bar{\rho}$  to be even under reversal of both the magnetic field and the magnetic order.

In an isotropic material, the OMR contribution is present only in longitudinal resistivity. However, OMR can also manifest in the transverse resistivity if the symmetry of the crystal is low enough: For a general current direction, the OMR contribution to transverse resistivity will necessarily exist in an anisotropic crystal where the longitudinal OMR is different along two directions, as a result of the linearity of the resistivity. This typically is not observed in an experiment because the anisotropy of the resistivity is weak, the electrical current is often applied along one of the main crystallographic axes, or the crystallinity of the measured samples is insufficient [15]. When the transverse OMR is negligible, the even component of the transverse resistivity can indicate whether AMR is present since AMR contributes both

to the diagonal and off-diagonal components of the resistivity tensor.

In a typical measurement of the anomalous Hall effect, the external magnetic field is swept perpendicular to the current direction. In such a scenario, AMR is often assumed not to contribute to the transverse resistivity which is justified for high-symmetry materials and the magnetization exactly following the external magnetic field. Below the saturation field, however, magnetization is not aligned with the external field even in a simple ferromagnet and the assumption is thus not valid. Moreover, it is usually not true in more complex materials with low symmetry, such as non-collinear antiferromagnets [16–18]. Therefore, the even component of transverse resistivity can also indicate the presence of AMR. Other even-in-field effects contributing to transverse resistivity have been considered in relation to non-centrosymmetric Berry curvature [19]. Furthermore, note that a quadratic-in-field contribution to transverse resistivity may arise when the anomalous and ordinary Hall angles are sizable [20].

From the experimental point of view, additional effects can result in an even contribution to transverse resistivity. One possible source is the geometrical misalignment of the transverse contacts with respect to the current direction (see Fig. 1a), which yields a contribution of longitudinal signal to transverse voltage. Since the longitudinal signal has typically an even symmetry with respect to the applied field, this artefact is also even. Unfortunately, the geometrical offset is almost unavoidable. Lithographically defined Hall bar microstructures are less sensitive to the contact misalignment artefacts as compared to the bulk crystal samples with hand-soldered contacts. However, even during a lithographical process, small imperfections might still arise from the resist or etching inhomogeneity and shadows. To suppress these geometrical artefacts, the even part of the field-sweep data is often removed [21, 22]. This approach isolates the dominant Hall signal that is straightforward to analyze. However, at the same time, part of the information is lost. Especially in materials with a complex magnetic structure, the even component of transverse resistivity can provide important information about their magnetic order.

In this paper, we discuss the symmetry of the experimentally measured transverse resistivity in both a simple ferromagnet and a complex compensated magnet. All experiments are performed with the magnetic field perpendicular to the electric current. We sweep the magnetic field and detect the voltage transverse and longitudinal to the applied electric current. We show that an even contribution to transverse resistivity can be present in per-

fectly aligned contacts, cannot be correlated to the longitudinal voltage, and may reflect the magnetic order. The structure of the paper is as follows: Firstly, we demonstrate possible artefacts arising from an intentional offset of the contacts in a conventional ferromagnet CoFeB. We propose an analysis scheme to remove these artefacts by defining a quantity independent of the geometrical offset, and we show that the remaining even component of transverse resistivity can be explained within the single domain Stoner–Wohlfarth model of a ferromagnet. Finally, we apply this approach to the compensated magnetic material Mn<sub>5</sub>Si<sub>3</sub> with a complex magnetic structure [22]. We show that the even component of transverse resistivity arises in the low spin symmetry state of Mn<sub>5</sub>Si<sub>3</sub> and cannot be correlated with the longitudinal resistivity. We interpret this component in terms of finite magnetic-order-dependent resistance in Mn<sub>5</sub>Si<sub>3</sub>.

#### II. SAMPLE PREPARATION AND EXPERIMENTAL SETUP

A ferromagnetic  $Co_{40}Fe_{40}B_{20}$  film with a thickness of 15 nm was deposited by magnetron sputtering on a single-crystal MgO (100) substrate using a Bestec UHV deposition system (with a sputtering pressure of  $3 \cdot 10^{-3}$  mbar). The magnetization of CoFeB is approximately  $1200 \,\mathrm{kA/m}$  at room temperature [23]. Thin films of  $\mathrm{Mn}_5\mathrm{Si}_3$  were grown by molecular beam epitaxy on intrinsic Si (111) substrates with a  $\mathrm{Mn}_5\mathrm{Si}_3$  thickness ranging from 12 to 20 nm depending on the sample [24].

Both CoFeB and  $Mn_5Si_3$  thin films were patterned into Hall bar microstructures using optical lithography and plasma etching. A detail of a microscope image of the Hall bar prepared on CoFeB is shown in Fig. 1a. This reference device consists of a set of Hall crosses where each pair of transverse contacts has a different artificial offset  $\delta$  of  $-10 \,\mu\text{m}$ ,  $-5 \,\mu\text{m}$ ,  $0 \,\mu\text{m}$ , and  $5 \,\mu\text{m}$ .

A scheme of the experiment geometry is shown in Fig. 1b. The external magnetic field was swept perpendicularly to the sample plane while measuring transverse voltages  $V_{yx}$  on multiple transverse contact pairs. Simultaneously, the longitudinal voltage  $V_{xx}$  was detected. All the presented magnetotransport data were obtained in an Oxford Instruments cryostat Integra AC with a variable-temperature insert equipped with two thermometers to monitor the sample base temperature with high precision. We use Keithley 2182 nanovoltmeters to detect  $V_{yx}$  and  $V_{xx}$ . A DC current was applied along the x-axis by a Keithley 2450 source

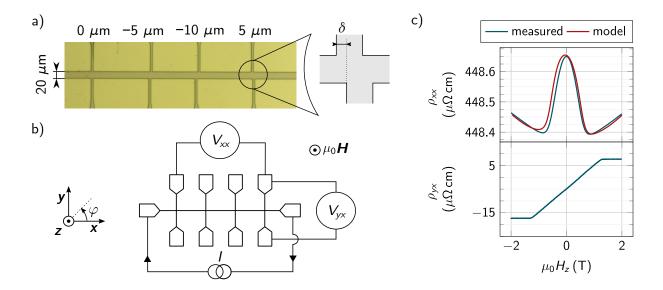


Figure 1. Reference CoFeB device: a) A microscope image of transverse contacts with an artificial offset of  $\delta$  in the range from  $-10 \,\mu\text{m}$  to  $5 \,\mu\text{m}$ , b) schematics of the measurement, c) an example of the dependence of longitudinal  $\rho_{xx}$  and transverse  $\rho_{yx}$  resistivity on an external magnetic field applied along z- direction at 100 K. The data are shown as measured for  $\delta = 0 \,\mu\text{m}$ , only the voltage was recalculated to the respective values of resistivity. The panel of longitudinal resistivity also includes the result of the Stoner–Wohlfarth model for the  $\rho_{xx}(H_z)$  dependence.

measure unit, and the transverse voltage was measured as a function of the applied out-ofplane magnetic field. An example of longitudinal and transverse resistivity data measured on a 15-nm CoFeB sample is shown in Fig. 1c: The main contributions to the longitudinal resistivity are from AMR and OMR, whereas the transverse resistivity is dominated by the anomalous Hall effect.

#### III. RESULTS

#### A. CoFeB reference sample

The crucial step of our proposed method is isolating odd or even components of the measured data with respect to the applied magnetic field. When considering a field-sweep experiment, i.e. a measurement of resistivity as a function of an external magnetic field magnitude, the even and odd components  $\rho^{\text{even}}$  and  $\rho^{\text{odd}}$  can be obtained as follows:

$$\rho_{\leftarrow}^{\text{even}}(H) = \frac{\rho_{\leftarrow}(H) + \rho_{\rightarrow}(-H)}{2}, \quad \rho_{\leftarrow}^{\text{odd}}(H) = \frac{\rho_{\leftarrow}(H) - \rho_{\rightarrow}(-H)}{2}, \tag{1}$$

where  $\rho_{\leftarrow}(H)$  and  $\rho_{\rightarrow}(H)$  are the subsets of the  $\rho$  data corresponding to either descending or ascending sweep direction (i.e. data taken for a decreasing or increasing magnetic field magnitude), which we introduced to account for eventual hysteresis. The corresponding  $\rho_{\rightarrow}^{\text{even}}(H)$  and  $\rho_{\rightarrow}^{\text{odd}}(H)$  can be obtained by interchanging  $\rho_{\leftarrow}(H)$  and  $\rho_{\rightarrow}(H)$  in Eq. (1). For clarity, the procedure is visualized in Appendix A.

The data measured on a CoFeB Hall bar for various offsets  $\delta$  is shown in Fig. 2. The first row corresponds to the measured transverse resistivity  $\rho_{yx}(H_z)$ : The dominant part of the field dependence is the odd component corresponding to the anomalous Hall effect (AHE) measured along the magnetic hard axis and, therefore, showing no hysteresis. The vertical offset of the data reflects the geometrical misalignment. There is also a clear even part, as seen in the second line, which shows the even component of transverse resistivity  $\rho_{yx}^{\text{even}}(H_z)$ . The even component depends on the geometrical offset as expected since it contains a contribution from longitudinal resistivity dominated by OMR and AMR. We, therefore, introduce a quantity that is independent of the geometrical misalignment  $\rho_{\perp}^{\text{even}}$ :

$$\rho_{\perp}^{\text{even}}(H) = \rho_{yx}^{\text{even}}(H) - \alpha \cdot \rho_{xx}^{\text{even}}(H). \tag{2}$$

In this definition, the quantity  $\alpha = \langle \rho_{yx}^{\text{even}} \rangle / \langle \rho_{xx}^{\text{even}} \rangle$  is the ratio of the  $\rho_{yx}^{\text{even}}$  and  $\rho_{xx}^{\text{even}}$  mean values with respect to the field H.  $\alpha$  quantifies the projection of longitudinal resistivity in the transverse resistivity. By subtracting the even component of longitudinal resistivity  $\rho_{xx}^{\text{even}}$  scaled by  $\alpha$ , only the even component of transverse resistivity free of any geometrical misalignment and constant offset is left. Please note that the arithmetic mean is only one of many possibilities of quantifying the  $\rho_{yx}^{\text{even}}$  and  $\rho_{xx}^{\text{even}}$  in the definition of the  $\alpha$  coefficient. However, the choice does not influece the resulting  $\rho_{\perp}$  in our case, as the relative variations of  $\rho_{yx}^{\text{even}}(H)$  and  $\rho_{xx}^{\text{even}}(H)$  are small.

The last row of Fig. 2 reveals that  $\rho_{\perp}^{\text{even}}$  is identical for all transverse contacts as expected, and does not depend on the geometrical offset. Because in our polycrystalline sample the contribution of OMR is not expected in transverse resistivity, the origin of the remaining signal can be attributed to AMR. This is also in agreement with the saturation of  $\rho_{\perp}^{\text{even}}$  at high magnetic fields. We note that in our experimental geometry, transverse AMR would not

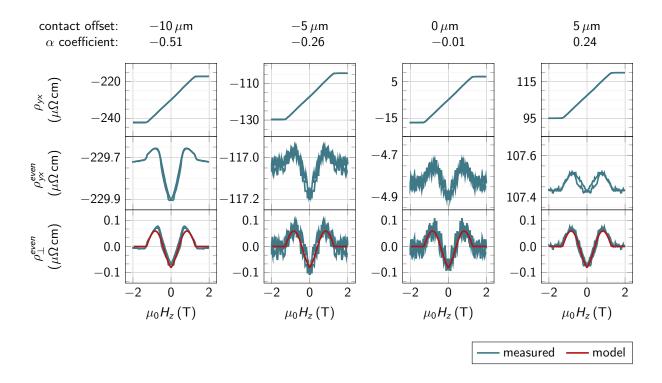


Figure 2. Field sweeps measured on a reference CoFeB device at 100 K using multiple contacts with different geometrical offset: The first row shows raw transverse data, the second row its even component, and the third row depicts the offset-independent quantity  $\rho_{\perp}^{\text{even}}$  with the corresponding  $\alpha$  coefficients shown in the header. The last row also shows a model for the even component of  $\rho_{yx}$ . For the  $\rho_{xx}$  data, see Fig. 1c.

be expected, and thus our data reveals that the magnetization does not follow the external magnetic field entirely. The field dependence of the longitudinal AMR and the transverse AMR in our polycrystalline sample is distinct (compare Fig. 1c and the last row of Fig. 2) because the former solely depends on the angle between magnetization and current direction, whereas the latter also on the in-plane projection of the magnetization.

In order to describe the origin of  $\rho_{\perp}^{\text{even}}$  in CoFeB, we implemented a single domain model. We obtain the uniaxial anisotropy constant by fitting the dependence of longitudinal resistivity on the applied magnetic field direction within the Stoner-Wohlfarth model (see for example [25]). To describe the complex trajectory of the magnetization in the vicinity of zero magnetic field, we allow the magnetization to develop a finite projection in the sample plane described by the angles  $\theta$  and  $\varphi$ . The angle  $\theta$  describes the angle between the z-axis and the magnetization and the inplane direction is determined by  $\varphi$  as defined in

Fig. 1b. The magnetization is aligned with the out-of-plane external magnetic field at high magnetic fields. Once the magnetic field is reduced below the anisotropy field (1.6 T, see Fig. 1c), the magnetization vector continuously cants towards the sample plane, and it concomitantly changes its in-plane orientation constrained by the weak in-plane anisotropy. In this notation, we calculate transverse resistivity  $\rho_{yx}$  as follows:

$$\rho_{ux}(\theta,\varphi) = a_1 \cos \theta + a_2 \cos^3 \theta + a_3 \sin^2 \theta \sin \varphi \cos \varphi, \tag{3}$$

where  $a_{1,2,3}$  are coefficients which we identified with the following values using the Stoner-Wohlfarth model:  $a_1 = 11.62 \,\mu\Omega$ cm,  $a_2 = -0.28 \,\mu\Omega$ cm,  $a_3 = 1.00 \,\mu\Omega$ cm. The first two terms in Eq. (3) describe the anomalous Hall effect and its anisotropy [26], whereas the  $a_3$  coefficient quantifies the contribution of transverse AMR [2]. The value of  $a_3$  we found falls within the range typical for CoFeB alloys (for example,  $Co_{60}Fe_{20}B_{20}$  was reported to have  $2.5 \,\mu\Omega$ cm [27]). The finite magnetization projection in the sample plane is required to understand the field dependence of  $\rho_{\perp}^{\text{even}}$ , as shown in Fig. 2 (the red line is the model). Although the longitudinal and the transverse signal shape is seemingly very different, the same model can also fit the longitudinal AMR (see Fig. 1c). Both the measured data and the modelling confirm that the AMR is non-zero, although the magnetic field is perpendicular to the current and voltage detection direction (the Hall geometry).

#### B. Application to Mn<sub>5</sub>Si<sub>3</sub>

In the previous section, we have shown that in the Hall geometry, the even component of transverse resistivity can be present even in a common ferromagnet regardless of the geometrical offset. In the case of CoFeB, a simple polycrystalline ferromagnet, it originates in the AMR. The AMR in ferromagnets can be relatively easily measured and identified because it saturates with the saturation of the magnetization. The AMR is, however, not well understood and described in material systems with a more complex spin structure. In many cases, it is challenging to distinguish the AMR from the OMR. This is mainly because magnetic order in more complex magnets does not necessarily saturate in an achievable magnetic field, and, therefore, the saturation of the AMR is often not reached. If we apply current along a high-symmetry crystallographic axis, the ordinary magnetoresistance does not contribute to the even part of the transverse resistivity after removing the geometrical

offset ( $\rho_{\perp}^{\text{even}}$ ). The quantity  $\rho_{\perp}^{\text{even}}$  could, therefore, serve as a good indicator of more complex magnetoresistance signals. In the following, we test this approach in a compensated magnetic system with a complex spin structure and phase transitions —  $Mn_5Si_3$  [22, 28]. Our  $Mn_5Si_3$  films show a transition between a low-temperature non-collinear magnetic phase AM1 and a high-temperature collinear magnetic phase AM2 at 70 K. The films become paramagnetic at 240 K [22]. It was shown that due to their particular spin and crystal symmetry, the epitaxial  $Mn_5Si_3$  thin films are altermagnetic candidates [22, 29] and can exhibit anomalous Hall effect despite their vanishing magnetization [22]. Interestingly, the Hall effect (the odd part of the transverse voltage) has the same magnitude in the whole temperature range (10–240 K) and, therefore, is insensitive to the magnetic phase transitions [22]. Such behaviour is distinct from bulk and polycrystalline  $Mn_5Si_3$  where the anomalous Hall effect is present only in their non-collinear magnetic phase below  $\approx 60$  K [30]. Furthermore, these systems show a Néel temperature of 100 K which is very different from the one in our epitaxial layers

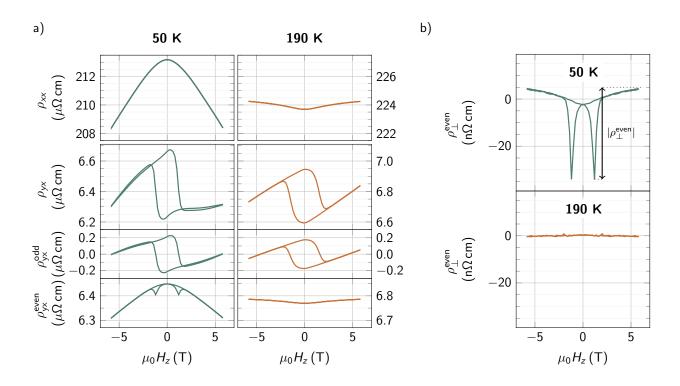


Figure 3. Field sweeps measured on  $Mn_5Si_3$  epitaxial films at 50 K and 190 K: a) Measured longitudinal and transverse resistivity  $\rho_{xx}$  and  $\rho_{yx}$  for two temperatures. Odd and even components of  $\rho_{yx}$  with respect to the applied magnetic field are separated. b) Misalignment-independent quantity  $\rho_{\perp}^{\text{even}}$ .

[30, 31].

An example of transverse resistivity  $\rho_{yx}(H_z)$  measured at 190 K and 50 K is shown in Fig. 3a, together with its odd and even components with respect to the magnetic field. For illustration, also the longitudinal resistivity  $\rho_{xx}(H_z)$  is included in Fig. 3a. It can be seen that the transverse resistivity has a clear even component which is pronounced in the low temperature (low spin symmetry) regime. To remove the effect of geometrical misalignment, we use the approach described above, and we evaluate the offset-independent value  $\rho_{\perp}^{\text{even}}$ . This component is substantially higher at 50 K than at 190 K, as shown in Fig. 3b. The hysteresis behaviour observed in the  $\rho_{\perp}^{\text{even}}$  highlights its difference to the  $\rho_{xx}$ . In the hexagonal lattice of Mn<sub>5</sub>Si<sub>3</sub>, in the absence of the magnetic order, and for current along a high symmetry direction, the transverse OMR is not allowed by symmetry [32]. Therefore the  $\rho_{\perp}^{\text{even}}$  must arise from the magnetic properties of the material.

This approach reveals its potential if we apply it to a set of temperatures and samples.

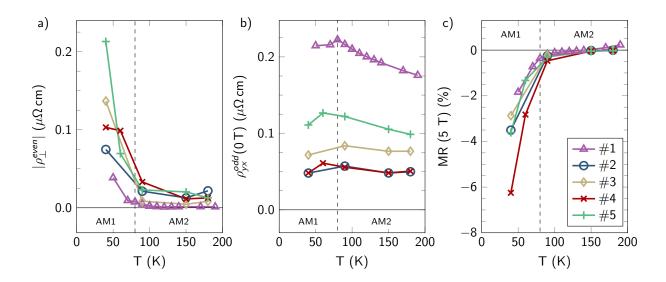


Figure 4. Temperature dependence of a) the maximum change of the misalignment-independent quantity  $\rho_{\perp}^{\text{even}}(H)$  as defined in Fig. 3b, b) the magnitude of spontaneous Hall resistivity, i.e. the value of  $\rho_{yx}^{\text{odd}}$  in zero magnetic field, and c) magnetoresistance measured at 5 T for five Mn<sub>5</sub>Si<sub>3</sub> samples. Note the different temperature dependence of the usual  $\rho_{yx}$  treatment (panel b) and the method we propose (panel a). The individual samples differ by their crystal quality and the proportion of a spurious MnSi phase on the Mn<sub>5</sub>Si<sub>3</sub>/Si interface. The data in Fig. 3a are from the sample #1.

We evaluated the  $\rho_{\perp}^{\text{even}}$  in the temperature range of 10–190 K for several Mn<sub>5</sub>Si<sub>3</sub> samples that differ in their parameters, such as layer thickness or composition of spurious phases [22]. In Fig. 4a, we show the absolute amplitude of the  $\rho_{\perp}^{\text{even}}(H_z)$  dependence extracted directly from the detected hysteresis loops (see Fig. 3b) for different sample temperatures. It can be seen that the signal is sizable in the AM1 phase (5–70 K), where low spin symmetry is expected. Unlike the usual treatment of the transverse resistivity, i.e. considering the spontaneous or saturated Hall signal  $\rho_{yx}^{\text{odd}}$  (see Fig. 4b), our even signal  $\rho_{\perp}^{\text{even}}$  reflects the phase transition precisely, and is vanishingly small in the AM2 phase (70–240 K). Note that we include only data measured below 190 K to avoid even-in-field contributions from the finite conductivity of the silicon substrate above this temperature. Although the general trend of increased  $\rho_{\perp}^{\text{even}}$  in the AM1 phase is common for all samples, we stress that not all the samples exhibit the hysteretic behaviour shown in Fig. 3b.

The presence of magnetoresistance related to the magnetic order would be, in principle, in agreement with the longitudinal resistivity  $\rho_{xx}$  signals which reveal a similar temperature dependence (see Fig. 4c). Interestingly, when comparing multiple samples,  $\rho_{xx}$  and  $\rho_{\perp}^{\text{even}}$  cannot be correlated as follows from Fig. 4: The maximal value of the longitudinal magnetoresistance was observed in a different sample than the maximum of  $\rho_{\perp}^{\text{even}}$ . In a ferromagnet, this difference could be caused by appreciable crystalline AMR [33]. Furthermore, the different magnetic domain structures occurring in different samples cannot be ruled out. When attributed to AMR,  $\rho_{\perp}^{\text{even}}$  and its complex behaviour may be related to the particular magnetic structure of Mn<sub>5</sub>Si<sub>3</sub>: Below the Néel temperature, Mn<sub>5</sub>Si<sub>3</sub> shows only four magnetically ordered Mn atoms in a unit cell with the remaining six Mn atoms being disordered and with more Mn atoms getting ordered in the low-temperature AM1 phase. These disordered moments might then contribute to the even-in-field transverse signal via AMR if ordered by external magnetic field.

#### IV. SUMMARY

In this work, we discussed the origin of the even-in-field component of transverse resistivity, and we showed that the transverse magnetotransport signals need to be evaluated carefully. In the Hall geometry, the even part of transverse resistivity does not necessarily result from measurement artefacts, such as the geometrical misalignment. We define the

even part of the transverse resistivity  $\rho_{\perp}^{\text{even}}$  which is independent of the geometrical offset. The  $\rho_{\perp}^{\text{even}}$  can contain useful information about the existence of the AMR or even about the nature of the magnetic structure. We demonstrate this approach in a simple polycrystalline ferromagnet, where we approximate the  $\rho_{\perp}^{\text{even}}$  by a single domain model. We show that longitudinal and transverse AMR measured in the magnetic field sweep do not have to show the same magnitude and symmetry due to the complex magnetization trajectory.

We further test this approach on a compensated magnet with a complex magnetic structure —  $Mn_5Si_3$ . We isolate  $\rho_{\perp}^{even}$  signals in a series of measurements, and we show that the  $\rho_{\perp}^{even}$  can serve as a probe of the magnetic phase transition between its individual magnetic orderings that are hidden in the conventional magnetic characterization methods. The different magnitude of  $\rho_{\perp}^{even}$  in low- and high-temperature magnetic phases of  $Mn_5Si_3$  may reflect the proposed magnetic ordering of the thin films [22].

Compared to other magnetotransport methods used for the confirmation of the magnetic phase transitions (such as the measurement of the resistivity temperature dependence),  $\rho_{\perp}^{\text{even}}$  appears to be a more robust indicator as it is less prone to be influenced by e.g. structural transitions in the material.

### Appendix A: Extraction of odd and even components of the resistivity field dependence

The procedure of separating odd- and even-in-field components of a field-sweep experiment which we describe by Eq. (1) is illustrated in Fig. A.1 on  $\rho_{xy}$  measured in our Mn<sub>5</sub>Si<sub>3</sub> sample at 50 K. Panel a) shows the raw data separated into two subsets  $\rho_{\leftarrow}$  and  $\rho_{\rightarrow}$  corresponding to descending (blue) and ascending (red) magnetic field, respectively. For the odd-in-field component in panel b), we separately calculate its field-descending  $\rho_{\leftarrow}^{\text{odd}}$  (cyan) and field-ascending  $\rho_{\rightarrow}^{\text{odd}}$  (magenta) sections. The  $\rho_{\leftarrow}^{\text{odd}}$  section is determined by directly applying Eq. (1), whereas  $\rho_{\rightarrow}^{\text{odd}}$  is defined by interchanging  $\rho_{\leftarrow}$  and  $\rho_{\rightarrow}$  in the equation. For the even-in-field component in panel c), we use an analogous procedure to find  $\rho_{\leftarrow}^{\text{even}}$  (yellow) and  $\rho_{\rightarrow}^{\text{even}}$  (green).

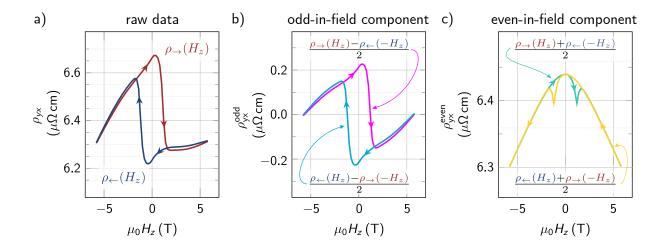


Figure A.1. Extraction of odd-in-field and even-in-field contributions from field-sweep data as illustrated on a  $\rho_{yx}(H_z)$  sweep measured on a  $\mathrm{Mn}_5\mathrm{Si}_3$  thin film at 50 K. a) Transverse resistivity field dependence as measured. The figure shows the definition of  $\rho_{\leftarrow}$  and  $\rho_{\rightarrow}$  encoded in color. b) The odd-in-field component of the dependence in panel a). c) The even-in-field component of the dependence in panel a).

We acknowledge CzechNanoLab Research Infrastructure supported by MEYS CR (LM 2018110) and LNSM-LNSpin. We also acknowledge the Grant Agency of the Czech Republic Grant No. 22-17899K, the EU FET Open RIA Grant No. 766566, and the French national research agency (ANR), grant No. ANR-20-CE92-0049-01. Financial support was provided by the Deutsche Forschungsgemeinschaft (DFG, German Research Foundation) via Project-ID 445976410 GO 944/8 and 425217212 SFB 1432, and 45976410. The study was supported by Charles University, project GA UK No. 266723. H. R. is funded by Czech Science Foundation grant 22-17899K. D.K. acknowledges the support from the Czech Academy of Sciences (project No. LQ100102201).

[1] N. Nagaosa, J. Sinova, S. Onoda, A. H. MacDonald, and N. P. Ong, Anomalous Hall effect, Reviews of Modern Physics 82, 1539 (2010).

- [2] P. Ritzinger and K. Výborný, Anisotropic magnetoresistance: materials, models and applications, Royal Society Open Science **10**, 230564 (2023).
- [3] Y. Akgoz and G. Saunders, Space-time symmetry restrictions on the form of transport tensors.
   I. Galvanomagnetic effects, Journal of Physics C: Solid State Physics 8, 1387 (1975).
- [4] M. Seemann, D. Ködderitzsch, S. Wimmer, and H. Ebert, Symmetry-imposed shape of linear response tensors, Physical Review B **92**, 155138 (2015).
- [5] C. Chien, The Hall effect and its applications (Springer Science & Business Media, New York, 1980).
- [6] C.-Z. Chang, J. Zhang, X. Feng, J. Shen, Z. Zhang, M. Guo, K. Li, Y. Ou, P. Wei, L.-L. Wang, Z.-Q. Ji, Y. Feng, S. Ji, X. Chen, J. Jia, X. Dai, Z. Fang, S.-C. Zhang, K. He, Y. Wang, L. Lu, X.-C. Ma, and Q.-K. Xue, Experimental observation of the quantum anomalous Hall effect in a magnetic topological insulator, Science 340, 167 (2013).
- [7] N. Kiyohara, T. Tomita, and S. Nakatsuji, Giant anomalous Hall effect in the chiral antiferromagnet Mn<sub>3</sub>Ge, Physical Review Applied **5**, 064009 (2016).
- [8] L. Smejkal, R. Gonzalez-Hernandez, T. Jungwirth, and J. Sinova, Crystal time-reversal symmetry breaking and spontaneous Hall effect in collinear antiferromagnets, Science Advances 6, eaaz8809 (2020).
- [9] B. Gbel, I. Mertig, and O. A. Tretiakov, Beyond skyrmions: Review and perspectives of

- alternative magnetic quasiparticles, Physics Reports 895, 1 (2021).
- [10] G. Kimbell, C. Kim, W. Wu, M. Cuoco, and J. W. A. Robinson, Challenges in identifying chiral spin textures via the topological Hall effect, Communications Materials 3, 19 (2022).
- [11] M. Isasa, S. Vlez, E. Sagasta, A. Bedoya-Pinto, N. Dix, F. Snchez, L. E. Hueso, J. Fontcuberta, and F. Casanova, Spin Hall magnetoresistance as a probe for surface magnetization in Pt/CoFe<sub>2</sub>O<sub>4</sub> bilayers, Physical Review Applied 6, 034007 (2016).
- [12] L. Néel, Magnetism and the local molecular field, in Nobel Lectures Physics 1963-1970, edited by Elsevier (1972).
- [13] V. A. Zyuzin, Linear magnetoconductivity in magnetic metals, Physical Review B 104, L140407 (2021).
- [14] Y. Wang, P. A. Lee, D. Silevitch, F. Gomez, S. Cooper, Y. Ren, J.-Q. Yan, D. Mandrus, T. Rosenbaum, and Y. Feng, Antisymmetric linear magnetoresistance and the planar Hall effect, Nature communications 11, 1 (2020).
- [15] F. Zeng, Y. Ren, Y. Li, J. Zeng, M. Jia, J. Miao, A. Hoffmann, W. Zhang, Y. Wu, and Z. Yuan, Intrinsic mechanism for anisotropic magnetoresistance and experimental confirmation in Co<sub>x</sub>Fe<sub>1-x</sub> single-crystal films, Physical Review Letters 125, 097201 (2020).
- [16] I. Fina, X. Marti, D. Yi, J. Liu, J. H. Chu, C. Rayan-Serrao, S. Suresha, A. B. Shick, J. elezn, T. Jungwirth, J. Fontcuberta, and R. Ramesh, Anisotropic magnetoresistance in an antiferromagnetic semiconductor, Nature Communications 5, 4671 (2014).
- [17] H. Wang, C. Lu, J. Chen, Y. Liu, S. L. Yuan, S.-W. Cheong, S. Dong, and J.-M. Liu, Giant anisotropic magnetoresistance and nonvolatile memory in canted antiferromagnet Sr<sub>2</sub>IrO<sub>4</sub>, Nature Communications 10, 2280 (2019).
- [18] V. Sharma, R. Nepal, and R. C. Budhani, Planar hall effect and anisotropic magnetoresistance in thin films of the chiral antiferromagnet Mn3Sn, Physical Review B **108**, 144435 (2023).
- [19] M.-X. Yang, H.-D. Li, W. Luo, B. Miao, W. Chen, D. Xing, et al., Topological linear magnetoresistivity and thermoconductivity induced by noncentrosymmetric berry curvature, Physical Review B 107, 165130 (2023).
- [20] J. Zhao, B. Jiang, J. Yang, L. Wang, H. Shi, G. Tian, Z. Li, E. Liu, and X. Wu, Magneto-transport induced by anomalous hall effect, Physical Review B **107**, L060408 (2023).
- [21] J. P. DeGrave, D. Liang, and S. Jin, A general method to measure the Hall effect in nanowires: Examples of FeS<sub>2</sub> and MnSi, Nano Letters **13**, 2704 (2013).

- [22] H. Reichlová, R. Lopes Seeger, R. González-Hernández, I. Kounta, R. Schlitz, D. Kriegner, P. Ritzinger, M. Lammel, M. Leiviskä, V. Petříček, et al., Macroscopic time reversal symmetry breaking arising from antiferromagnetic Zeeman effect, arXiv e-prints, 2012.15651 (2020).
- [23] J. Cho, J. Jung, K.-E. Kim, S.-I. Kim, S.-Y. Park, M.-H. Jung, and C.-Y. You, Effects of sputtering Ar gas pressure in the exchange stiffness constant of Co<sub>40</sub>Fe<sub>40</sub>B<sub>20</sub> thin films, Journal of Magnetism and Magnetic Materials 339, 36 (2013).
- [24] I. Kounta, H. Reichlova, D. Kriegner, R. L. Seeger, A. Badura, M. Leiviska, A. Boussadi, V. Heresanu, S. Bertaina, M. Petit, et al., Competitive actions of MnSi in the epitaxial growth of Mn<sub>5</sub>Si<sub>3</sub> thin films on Si (111), Physical Review Materials 7, 024416 (2023).
- [25] P. Ritzinger, H. Reichlova, D. Kriegner, A. Markou, R. Schlitz, M. Lammel, D. Scheffler, G. H. Park, A. Thomas, P. Středa, et al., Anisotropic magnetothermal transport in Co<sub>2</sub>MnGa thin films, Physical Review B 104, 094406 (2021).
- [26] H. Zhang, S. Blügel, and Y. Mokrousov, Anisotropic intrinsic anomalous hall effect in ordered 3d Pt alloys, Physical Review B 84, 024401 (2011).
- [27] K. M. Seemann, F. Freimuth, H. Zhang, S. Blügel, Y. Mokrousov, D. E. Bürgler, and C. M. Schneider, Origin of the planar hall effect in nanocrystalline Co<sub>60</sub>Fe<sub>20</sub>B<sub>20</sub>, Phys. Rev. Lett. 107, 086603 (2011).
- [28] C. Sürgers, G. Fischer, P. Winkel, and H. v. Löhneysen, Large topological hall effect in the non-collinear phase of an antiferromagnet, Nature communications 5, 3400 (2014).
- [29] L. Šmejkal, J. Sinova, and T. Jungwirth, Emerging research landscape of altermagnetism, Physical Review X 12, 040501 (2022).
- [30] C. Sürgers, W. Kittler, T. Wolf, and H. v. Löhneysen, Anomalous hall effect in the noncollinear antiferromagnet Mn5Si3, AIP Advances 6, 055604 (2016).
- [31] N. Biniskos, F. dos Santos, K. Schmalzl, S. Raymond, M. dos Santos Dias, J. Persson, N. Marzari, S. Blügel, S. Lounis, and T. Brückel, Complex magnetic structure and spin waves of the noncollinear antiferromagnet Mn5Si3, Physical Review B 105, 104404 (2022).
- [32] S. V. Gallego, J. Etxebarria, L. Elcoro, E. S. Tasci, and J. M. Perez-Mato, Automatic calculation of symmetry-adapted tensors in magnetic and non-magnetic materials: a new tool of the Bilbao Crystallographic Server, Acta Crystallographica Section A 75, 438 (2019).
- [33] We take MR at 5 T as shown in the top panels of Fig. 3a as an estimate of magnetic-order-dependent magnetoresistance in our system with complex magnetic structure.